Field trial over 820 km installed SSMF and its potential Terabit/s superchannel application with up to 57.5-Gbaud DP-QPSK transmission

Tianhua Xu[a,b,c*], Jie Li[d], Gunnar Jacobsen[c,d], Sergei Popov[c], Anders Djupsjöbacka[d], Richard Schatz[c], Yimo Zhang[a], Polina Bayvel[b]

[a]Tianjin University, Tianjin, 300072, China

[b]University College London, London, WC1E7JE, United Kingdom

[c]Royal Institute of Technology, Stockholm, SE-16440, Sweden

[d]Acreo Swedish ICT AB, Electrum 236, Stockholm, SE-16440, Sweden

* Corresponding author: Tianhua Xu

Post address: Department of Electronic and Electrical Engineering, Faculty of Engineering, University College London, London, United Kingdom, WC1E 7JE

Tel: +44-7709662611

Fax: +44-2076793843

E-mail address: xutianhua@tju.edu.cn, tianhua.xu@ucl.ac.uk

ABSTRACT

In this paper, we report the result of a field trial of 56-Gbaud (224-Gbit/s) and 57.5-Gbaud (230-Gbit/s) dual-polarization quadrature phase shift keying (DP-QPSK) coherent optical transmission over 820 km installed standard single mode fiber (SSMF). Offline digital signal processing (DSP) was applied for signal recovery and bit-error-rate (BER) counting in our field trial experiments, and BER performance well below the 7% overhead hard-decision forward error correction (FEC) error-free threshold (4.5×10^{-3}) at 2^{31}-1 pseudo random bit sequence (PRBS) pattern length has been achieved, with the best achievable BERs of 2×10^{-4} (56-Gbaud) and 3×10^{-4} (57.5-Gbaud), respectively. In parallel a 1.15-Tbit/s (5×230-Gbit/s) quasi-Nyquist spaced wavelength division multiplexing (WDM) superchannel transmission over the same 820 km optical field link (FL) was also investigated through numerical simulations based on the same 57.5-Gbaud DP-QPSK signal using 1% roll-off Nyquist pulse shaping with 60-GHz channel spacing, and the results indicate that the BER performance well below the 7% overhead hard-decision FEC error-free threshold (4.5×10^{-3}) for the 1.15-Tbit/s DP-QPSK superchannel transmission can be achieved.

Key words: Coherent optical transmission, digital signal processing, field trial, optical fiber communication, quadrature phase shift keying

PACS: 42.25.Kb, 42.79.Sz

1. Introduction

Coherent optical detection enables advanced multi-level modulation formats and powerful digital signal processing (DSP), and can therefore significantly increase the spectral efficiency and the transmission capacity in fiber communication systems [1-5]. In addition, transmission system impairments including chromatic dispersion (CD), polarization mode dispersion (PMD), laser phase noise (PN), and fiber nonlinearities (FNLs) can also be compensated effectively by using DSP in the electrical domain [6-14]. Coherent transmission has, thus, become a most promising technology for the new-generation high capacity optical fiber networks. Since the first generation 100-Gbit/s coherent transmission system was commercialized, research has now been focused on investigating new solutions to enhance the transmission capacity to 400-Gbit/s - 1-Tbit/s and beyond. One approach is to use phase-locked optical sub-carriers to generate the so-called “superchannels”, which can transmit Nyquist (or quasi-Nyquist) spectral-spaced wavelength division multiplexing (WDM) channels using Nyquist pulse shaping (NPS) techniques [15-19]. For a fixed overall capacity (e.g. 1-Tbit/s), the number of the transmitter (Tx), the receiver (Rx), and the DSP setups depends on the tributary capacity of each sub-carrier in the superchannel transmission system, the higher tributary sub-carrier capacity the fewer hardware devices required for such systems. This can be realized by either raising the tributary data symbol rate or by employing a higher-order modulation format. It has been verified that [19,20], keeping the same tributary capacity, the system using a lower-order modulation format and a higher symbol rate will have a better tolerance to the fiber nonlinearities than the system using a higher-order modulation format and a lower symbol rate. The compensation of fiber nonlinearities is generally much more complex than other linear DSP operations, which becomes current key limitation for implementing the real-time digital receivers. Therefore, the use of a higher symbol rate will be a more promising option, with the development of analog-to-digital converters (ADCs) and DSP hardware.

Previously, high symbol rate single carrier (SC) optical transmission using dual-polarization quadrature phase shift keying (DP-QPSK) at 56-Gbaud had been demonstrated in a recirculating loop experiment using standard single mode fiber (SSMF) [21,22]. DP-QPSK systems at 80-Gbaud and 107-Gbaud had also been demonstrated using the ultra-large area fiber (ULAF) with Raman amplification [23-26]. In all these demonstrations the pseudo random bit sequence (PRBS) pattern lengths in the Tx were limited to 2^{15}-1 [21-26].

We have previously reported some initial results of a 57.5-Gbaud DP-QPSK field transmission experiment [27]. In this paper, we significantly extend that work to describe the details of the field trial experiments at the rates of 56-Gbaud and 57.5-Gbaud over an 820 km field-installed SSMF link, with erbium doped fiber amplifiers (EDFAs) only. Numerical simulations for Terabit/s superchannel transmission are also described. In the field trials, the signal recovery and BER measurement were both applied offline, while the DSP block was updated after each processing. All the tributary PRBS data at 56-Gbit/s and 57.5-Gbit/s had the pattern lengths of 2^{31}-1, giving a single carrier bit rate of 224-Gbit/s and 230-Gbit/s for the DP-QPSK transmission, respectively. BER performance well below the 7% overhead hard-decision forward error correction (FEC) error-free threshold (4.5×10^{-3}) have been achieved [28], with the best achievable BERs of 2×10^{-4} (56-Gbaud) and 3×10^{-4}

(57.5-Gbaud), respectively. In addition, to explore the potential of this system, numerical simulations of a 5-channel DP-QPSK quasi-Nyquist spaced WDM superchannel, with 57.5-Gbaud subcarriers, spaced by 60-GHz, were carried out over the same 820 km optical field link (FL), with an overall capacity of 1.15-Tbit/s. Simulation results indicate that the BER performance well below the 7% overhead hard-decision FEC error-free threshold (4.5×10^{-3}) can be achieved in the 1.15-Tbit/s DP-QPSK superchannel transmission.

2. Transmission experiments

2.1 Experimental setup and field link

Figure 1 shows the experimental setup for the 56-Gbaud and the 57.5-Gbaud DP-QPSK coherent optical transmission over the 820 km installed SSMF. The setup consisted of the DP-QPSK transmitter, the coherent receiver and the 820 km SSMF field link with in-line EDFAs.

Fig. 1. Experimental setup and field link of the DP-QPSK coherent transmission over 820 km installed SSMF in Sweden.

In the transmitter, a tunable external-cavity laser (ECL) at 1552.5 nm with ~100 kHz linewidth was employed as the light source. The tributary PRBS data (56-Gbit/s or 57.5-Gbit/s) were generated from a pattern generator with a PRBS pattern length of 2^{31}-1, amplified by the broadband electrical amplifiers (operated in the saturated mode with an input signal peak-to-peak swing of 1 V), then applied to an integrated quadrature amplitude modulation (QAM) transmitter unit (SHF 46213D, I-Q modulator: 3-dB bandwidth >25 GHz, V_π of ~3.5 V) to generate the (56-Gbaud or 57.5-Gbaud) QPSK signal. The polarization multiplexing was implemented using an optical polarization multiplexer, where the single polarization (SP) QPSK signal from the QAM transmitter unit was split equally first by a polarization beam splitter (PBS), delayed in one polarization branch (by ~20 ns), and then recombined with another polarization beam combiner (PBC).

At the receiver, an Agilent N4391A optical modulation analyzer (OMA) using a 4-channel 33 GHz & 80-GSample/s real-time sampling oscilloscope was employed to recover and analyze the received signal. The incorporated local oscillator (LO) in the OMA was a tunable ECL with ~100 kHz linewidth, and the balanced detection had a bandwidth of ~40 GHz. Signal recovery and impairments compensation were performed using offline DSP in OMA, which included the following elements: clock recovery was realized using digital re-sampling and retiming [29,30], CD compensation was carried out using overlap-save (OLS) based frequency domain equalizer (FDE) [6,31], polarization equalization was achieved using constant modulus algorithm (CMA) [1,9], and carrier phase estimation (CPE) was implemented using Viterbi & Viterbi algorithm [12]. No fiber nonlinearity compensation was applied in the DSP. The DSP and BER measurement were applied offline, while the BER was accumulated with the update of the data from the processed DSP-block (2048 symbols). All BERs were obtained from the comparison between the transmitted bits and the received bits.

In the bottom of Fig. 1, the 820 km installed FL comprised a series of G.652 SSMFs deployed in the eastern coastal area in Sweden, which interconnected seven nodes at Kista, Råsunda, Norrtälje, Östhammar, Gävle, Söderhamn and Hudiksvall. The DP-QPSK signals were transmitted from and received in the optical networking laboratory at Kista, and looped back in the farthest node, at Hudiksvall. Conventional EDFAs (with a noise figure of ~5.0 dB) were deployed in each node to control the launched signal optical power and compensate for the fiber losses. The chromatic dispersion of the installed 820 km SSMF based on the OMA measurement was ~14400 ps/nm, giving a CD coefficient of ~17.56 ps/(nm·km). The measured PMD of the 820 km SSMF based on Jones matrix analysis was ~4 ps, yielding a PMD coefficient of ~0.14 $ps/\sqrt{km}$. Both the CD and the PMD parameters were measured at the wavelength of 1552.5 nm. No optical dispersion compensation (ODC) was applied in the experiments.

To have a better optical signal-to-noise ratio (OSNR) sensitivity, here we used the coherently-detected (rather than differentially-coded) QPSK signal in the transmission system. Since both the transmitter and the LO lasers linewidths are very low (~100 kHz) and the signal symbol rate is very high (56-Gbaud or 57.5-Gbaud), the phenomenon of cycle slip seldom happens in such systems, when the CPE algorithm is well optimized. In practical applications, the cycle slip problem can be solved by using pilot-symbol assisted estimation or FEC coding techniques [32,33].

2.2 Experimental results and analysis

The I-Q constellations and the demodulated I/Q tributary eye-diagrams of the 56-Gbaud and the 57.5-Gbaud DP-QPSK signals are shown in Fig. 2, and their optical spectra are illustrated in Fig. 3, accordingly. Both cases before and after the 820 km field link transmission have been considered. In the back-to-back (BtB) case, the error vector magnitudes (EVMs) of the QPSK signals were relatively large at ~20-22% root-mean-square (RMS), because of the amplitude variations in the PRBS data (due to the imperfect frequency response and transition speed of the devices in the pattern generator) and the inter-symbol interference (ISI) induced by the bandwidth limited devices at these high symbol rates.

Fig. 2. Experimental DP-QPSK I-Q constellations and tributary (I/Q) eye-diagrams before and after 820 km field link (a) 56-Gbaud (b) 57.5-Gbaud.

Fig. 3. Experimental optical spectra of the 56-Gbaud and the 57.5-Gbaud DP-QPSK signals before and after 820 km field link transmission (0.07 nm resolution bandwidth).

The best achievable BERs for the 56-Gbaud and the 57.5-Gbaud DP-QPSK signals after the 820 km installed SSMF transmission, with different launched optical power in each SSMF span, are shown in Fig. 4. The BER performance of the 56-Gbaud and the 57.5-Gbaud signals were similar. It can be seen in Fig. 4 that for the optical launch powers in the range of 0.2 - 8.0 dBm, the measured BER was below the 7% overhead FEC error-free threshold (4.5×10^{-3}). The optimum launch power, for both the 56-Gbaud and the 57.5-Gbaud systems, was 4 dBm. This indicates that when the launched signal power was less than 4 dBm, the BER performance improved with the increment of launched signal power, corresponding to the OSNR improvement in the linear transmission region. When the optical power exceeded 4 dBm, the BER performance degraded due to the effect of fiber nonlinearities. Nevertheless, both the 56-Gbaud and the 57.5-Gbaud DP-QPSK signals had a robust (~7.8 dB in terms of signal power) tolerance margin to channel noise and fiber nonlinear distortions, when the launched optical power deviated from the optimum value (4 dBm).

Fig. 4. BER performance with different signal launch power in each SSMF span in the 820 km field link.

Figure 5 shows the measured BER versus the signal OSNR for the 56-Gbaud and the 57.5-Gbaud DP-QPSK transmission at the optimum launch optical signal power (4 dBm) in each SSMF span. It can be seen that little degradation of the 57.5-Gbaud signal can be observed as compared to the BER performance at 56-Gbaud, and the BER in both systems was well below the 7% overhead FEC error-free threshold (4.5×10^{-3}) after the transmission over the 820 km field-installed SSMF link. The penalty between the BtB and the 820 km field transmission at FEC error-free threshold (4.5×10^{-3}) was ~2.7 dB for both the 56-Gbaud and the 57.5-Gbaud transmission. The penalties were attributed mainly to the accumulated amplified spontaneous emission (ASE) noises in EDFAs and the fiber nonlinearities, which were not compensated in the DSP algorithms. These results demonstrate the potential and the performance of current field-deployed SSMF networks, if we upgrade the single channel capacity from 100-Gbit/s to 200-Gbit/s directly.

Fig. 5. BER versus OSNR at the optimum signal launch power (4 dBm for both 56-Gbaud and 57.5-Gbaud signals). The theoretical curve of BER versus OSNR performance is for the 57.5-Gbaud signal.

In the reported work [21], the best achievable BER for 56-Gbaud DP-QPSK signal in 820 km (roughly) recirculating SSMF loop experiment was ~9×10^{-5} (Q factor of ~11.5 dB in Fig. 4 in Ref. [21]). In our field trial, the best achievable BER for 56-Gbaud signal after 820 km installed SSMF transmission was 2×10^{-4}, which is moderately worse than the lab recirculating loop experiment. This can be attributed to the sub-optimization of EDFA optical launch power in the non-uniform fiber spans, the inaccuracy of dispersion compensation parameters, and the perturbation variant polarization dependent loss (PDL), etc., in the field trial. In the recirculating loop experiment, the transmission system parameters such as losses, dispersion, PMD, PDL, etc., are more stable than in the field trial, due to a good control on the temperature, the external force, the vibrations, etc. in the lab.

3. Superchannel transmission numerical simulations

To investigate the performance of a 1.15-Tbit/s (5×57.5-Gbaud) quasi-Nyquist spaced WDM superchannel transmission using the 57.5-Gbaud DP-QPSK signal over the same 820 km field link at a sub-carrier spacing of 60-GHz, numerical simulations were carried out using the split-step Fourier method. The schematic of the simulation setup is illustrated in Fig. 6. In the transmitter, a digital-to-analog convertor (DAC) with 6-bit resolution and a root-raised-cosine (RRC) filter with a roll-off of 1% were applied for the Nyquist pulse shaping. The effective number of bits (ENOB) in the DAC was controlled by introducing noise in the Tx, which was used to match the single-channel 57.5-Gbaud DP-QPSK BtB experimental result for emulating the same signal generator and linear penalty in our experiment, as the benchmark of the simulation work. To emulate an independent data transmission, the transmitted sequences in each sub-channel were de-correlated with a delay of 256 symbols, and the data were also de-correlated in the polarization multiplexing module with a delay of 2048 symbols in one polarization branch. In the receiver, a 5-th order Bessel filter with a 3-dB bandwidth of 33-GHz was applied to emulate the analog bandwidth of the receiver in the experiment. In the DSP modules, a matched filter (1% roll-off RRC filter) was applied to recover the Nyquist pulse shaped signal after the CD compensation. The structure of transmission fiber link was the same as the optical field link in the experiment (in Fig. 1), with the fiber nonlinear coefficient set as 1.35 W^{-1}/km. The step size in the split-step Fourier method based simulator was set to 0.1 km. The EDFA noise figure was set to 5.0 dB. The BER was evaluated based on 2^{18} bits with a PRBS pattern length of 2^{15}-1. All numerical simulations were carried out with a resolution of 16 samples/symbol to ensure that the digital bandwidth is twice higher than the transmission bandwidth.

Note that the PRBS pattern length was 2^{15}-1 in the simulation, which is different from the pattern length of 2^{31}-1 used in the experiment. It is because the number of total transmitted bits for BER evaluation in the simulation was 2^{18}, and this has already cost a lot of computation efforts, when a digital resolution of 16 samples/symbol and a step size of 0.1 km were employed to accurately emulate the propagation of the optical signal (with large bandwidth) in the fiber.

Fig. 6. Simulation setup for 5-channel quasi-Nyquist spaced DP-QPSK transmission (the 820 km field link is the same as the field link in Fig. 1). CDC: chromatic dispersion compensation, CPE: carrier phase estimation.

The spectra of the 5-channel 1% roll-off Nyquist pulse shaped DP-QPSK signal at 60-GHz spacing before and after the 820 km FL transmission are shown in Fig. 7, where the spectrum of the single-channel 57.5-Gbaud DP-QPSK signal without NPS (very similar to the corresponding experimental spectrum in Fig. 3) is also shown for reference.

Fig. 7. Simulated optical spectra of 5×57.5-Gbaud DP-QPSK Nyquist WDM superchannels before and after 820 km FL transmission.

The BER performance of 5-channel Nyquist pulse shaped 57.5-Gbaud DP-QPSK transmission with 1% roll-off under different optical launch power is shown in Fig. 8, where the single-channel 57.5-Gbaud DP-QPSK transmission with and without the 1% roll-off NPS are also illustrated. It can be seen that for the single-channel transmission, the optimum launch powers for both cases with and without NPS were 4 dBm. The Nyquist pulse shaping affected the performance in the linear region (at power levels lower than 4 dBm) slightly, while it distorted the performance in the nonlinear region (powers higher than 4 dBm) more significantly. For the WDM superchannel transmission, the BER performance degraded significantly due to the nonlinear interference in the fiber and the linear crosstalk among the sub-carriers. The optimum launch power per SSMF span was 9 dBm. The margin of launch power was ~6.8 dB (from 5.2 dBm to 12 dBm) to ensure the BER performing below the 7% overhead hard-decision FEC error-free threshold (4.5×10^{-3}).

Fig. 8. BER versus signal launch power in each SSMF span in the field link

(simulation).

It is noted that, without any NPS, the optimum signal power per channel in the conventional 5-channel WDM transmission should be nearly the same as the optimum signal power (4 dBm) in the single-channel DP-QPSK transmission [34]. Hence, the total optimum launch power in the conventional 5-channel WDM transmission system without NPS should be ~11 dBm, which corresponds to 4 dBm per channel. In Fig. 8, it can be seen that the optimum launch power (9 dBm) for 5-channel WDM superchannel transmission was less than the optimum launch power in conventional 5-channel WDM system without NPS. This is because the nonlinear distortion in the superchannel system is more severe due to the denser channel spacing.

The performance of the BER versus the OSNR at the optimum launch power (4 dBm for single-channel transmission with and without NPS, 9 dBm for WDM superchannel transmission) is shown in Fig. 9. It is found that the BER performance in the single-channel transmission was quite similar, both with and without Nyquist pulse shaping. However, compared to the single-channel DP-QPSK transmission, the WDM superchannel transmission had an OSNR penalty of ~1.2 dB in the BtB case, and an ONSR penalty of ~2 dB in the 820 km transmission case at the 7% overhead hard-decision FEC error-free threshold (4.5×10^{-3}). The numerical simulations give a promising prediction for our future work, where the Terabit/s superchannel transmission field trial will be carried out.

Fig. 9. BER versus OSNR at the optimum signal launch power in simulation (4 dBm for single-channel transmission with and without NPS, 9 dBm for WDM superchannel

transmission). The theoretical curve of BER versus OSNR performance is for the 57.5-Gbaud signal.

4. Conclusions

We experimentally demonstrated the single-carrier, coherent optical transmission over 820 km field-installed SSMF of DP-QPSK signal up to 57.5-Gbaud (56-Gbaud and 57.5-Gbaud), corresponding to a single channel capacity up to 230-Gbit/s. Offline DSP and BER measurement were applied with an iterative update of the processing block. The BER performance, well below the 7% overhead hard-decision FEC error-free threshold (4.5×10^{-3}) at the signal tributary PRBS pattern length of 2^{31}-1 had been achieved, with the best achievable BERs of 2×10^{-4} (56-Gbaud) and 3×10^{-4} (57.5-Gbaud), respectively. The significance of this work is to show the feasibility for upgrading the capacity of the commercial 100-Gbit/s DP-QPSK coherent transmission system directly to 200-Gbit/s and beyond.

Simulations to investigate the potential application of the 1.15-Tbit/s quasi-Nyquist spaced WDM superchannel transmission based on the same 57.5-Gbaud DP-QPSK signal over the same 820 km optical field link were carried out. The results showed that the BER performance well below the 7% overhead FEC error-free BER threshold (4.5×10^{-3}) for 5-channel 57.5-Gbaud DP-QPSK WDM transmission with 1% roll-off Nyquist pulse shaping at 60-GHz channel spacing can be achieved, highlighting the potential application of the 57.5-Gbaud DP-QPSK signal for Terabit/s superchannel transmission system, which will be implemented in our future field trial experiment.

Acknowledgements

This work is supported in part by KAW (Knut and Alice Wallenberg) Foundation, in part by UK Engineering and Physical Sciences Research Council (EPSRC) project UNLOC EP/J017582/1, and in part by FP7-PEOPLE-2012-IAPP (project GRIFFON, No. 324391).

References

[1] S. J. Savory, Digital coherent optical receivers: algorithms and subsystems, IEEE J. Sel. Top. Quant. Electron. 16 (2010) 1164-1179.

[2] G. Li, Recent advances in coherent optical communication, Adv. Opt. Photon. 1 (2009) 279-307.

[3] P. J. Winzer, R. J. Essiambre, Advanced modulation formats for high-capacity optical transport networks, J. Lightwave Technol. 24 (2006) 4711-4728.

[4] I. Garrett, G. Jacobsen, Phase noise in weakly coherent systems, IEE Proc. J. (Optoelectronics) 136 (1989) 159-165.

[5] E. Ip, A. P. T. Lau, D. J. F. Barros, J. M. Kahn, Coherent detection in optical fiber systems, Opt. Express 16 (2008) 753-791.

[6] T. Xu, G. Jacobsen, S. Popov, J. Li, E. Vanin, K. Wang, A. T. Friberg, Y. Zhang, Chromatic dispersion compensation in coherent transmission system using digital filters, Opt. Express 18 (2010) 16243-16257.

[7] T. Xu, G. Jacobsen, S. Popov, J. Li, K. Wang, A. T. Friberg, Normalized LMS digital filter for chromatic dispersion equalization in 112-Gbit/s PDM-QPSK coherent optical transmission system, Opt. Commun. 283 (2010) 963-967.

[8] M. Kuschnerov, F. N. Hauske, K. Piyawanno, B. Spinnler, M. S. Alfiad, A. Napoli, B. Lankl, DSP for coherent single-carrier receivers, J. Lightwave Technol. 27 (2009) 3614-3622.

[9] H. Zhu, X. Chen, W. Zhou, M. Zhang, An improvement on constant modulus algorithm for polarization demultiplexing in optical coherent receivers, Opt. Commun. 283 (2010) 4541-4545.

[10] S. Tsukamoto, K. Katoh, K. Kikuchi, Coherent demodulation of optical multilevel phase-shift-keying signals using homodyne detection and digital signal processing, IEEE Photon. Technol. Lett. 18 (2006) 1131-1133.

[11] G. Jacobsen, T. Xu, S. Popov, J. Li, A. T. Friberg, Y. Zhang, Receiver implemented RF pilot tone phase noise mitigation in coherent optical nPSK and nQAM systems, Opt. Express 19 (2011) 14487- 14494.

[12] A. J. Viterbi, A. M. Viterbi, Nonlinear estimation of PSK-modulated carrier phase with application to burst digital transmission, IEEE Trans. Inf. Theory 29 (1983) 543-551.

[13] Y. Gao, F. Zhang, L. Dou, Z. Chen, A. Xu, Electrical post-compensation of intrachannel nonlinearities in 10GBaud coherent QPSK transmission systems, Opt. Commun. 282 (2009) 992-996.

[14] J. Yang, S. Yu, M. Li, Z. Chen, Y. Han, W. Gu, An integral split-step Fourier method for digital back propagation to compensate fiber nonlinearity, Opt. Commun. 312 (2014) 80-84.

[15] I. Kaminow, T. Li, A. E. Willner, Optical fiber telecommunications VIA: components and subsystems, 6th ed., Academic Press, Oxford, 2013.

[16] H. C. Chien, J. Yu, Z. Jia, Z. Dong, X. Xiao, Performance assessment of noise-suppressed Nyquist-WDM for Terabit superchannel transmission, J.

Lightwave Technol. 30 (2012) 3965-3971.

[17] D. Qian, F. Yaman, Y. K. Huang, S. Zhang, E. Mateo, T. Inoue, Y. Inada, A. Hagisawa, T. Ogata, T. Wang, 512Gb/s DP-BPSK superchannel transmission over 7,200km DMF link with 1.43b/s/Hz spectral efficiency, Tech. Dig. Conf. Opt. Fiber Commun. (2013) JTh2A.

[18] M. A. Soto, M. Alem, M. A. Shoaie, A. Vedadi, C. S. Brès, L. Thévenaz, T. Schneider, Optical sinc-shaped Nyquist pulses of exceptional quality, Nature Commun. 4 (2013) 2898.

[19] G. Bosco, V. Curri, A. Carena, P. Poggiolini, F. Forghieri, On the performance of Nyquist-WDM Terabit superchannels based on PM-BPSK, PM-QPSK, PM-8QAM or PM-16QAM subcarriers, J. Lightwave Technol. 29 (2011) 53-61.

[20] P. Poggiolini, G. Bosco, A. Carena, V. Curri, Y. Jiang, F. Forghieri, The GN-model of fiber non-linear propagation and its applications, J. Lightwave Technol. 32 (2014) 694-721.

[21] P. J. Winzer, A. H. Gnauck, G. Raybon, M. Schnecker, P. J. Pupalaikis, 56-Gbaud PDM-QPSK: coherent detection and 2,500-km transmission, Tech. Dig. Conf. Eur. Opt. Commun. (2009) PD2.7.

[22] A. H. Gnauck, P. J. Winzer, G. Raybon, M. Schnecker, P. J. Pupalaikis, 10×224-Gb/s WDM transmission of 56-Gbaud PDM-QPSK signals over 1890 km of fiber, IEEE Photon. Technol. Lett. 22 (2010) 954-956.

[23] G. Raybon, P. J. Winzer, A. A. Adamiecki, A. H. Gnauck, A. Konczykowska, F. Jorge, J. Y. Dupuy, L. L. Buhl, C. R. Doerr, R. Delbue, P. J. Pupalaikis, All-ETDM 80-Gbaud (160-Gb/s) QPSK generation and coherent detection, IEEE Photon. Technol. Lett. 23 (2011) 1667-1669.

[24] G. Raybon, P. J. Winzer, A. A. Adamiecki, A. H. Gnauck, A. Konczykowska, F.

Jorge, J. Y. Dupuy, A. Sureka, C. Scholz, R. Delbue, P. J. Pupalaikis, L. L. Buhl, C. R. Doerr, S. Chandrasekhar, B. Zhu, D. W. Peckham, 8×320-Gb/s transmission over 5600 km using All-ETDM 80-Gbaud polarization multiplexed QPSK transmitter and coherent receiver, Tech. Dig. Conf. Opt. Fiber Commun. (2012) OTu2A.1.

[25] G. Raybon, A. Adamiecki, P. Winzer, C. Xie, A. Konczykowska, F. Jorge, J. Y. Dupuy, L. L. Buhl, C. Sethumadhavan, S. Draving, M. Grove, K. Rush, Single-carrier 400G interface and 10-channel WDM transmission over 4800 km using all-ETDM 107-Gbaud PDM-QPSK, Tech. Dig. Conf. Opt. Fiber Commun. (2013) PDP5A.

[26] G. Raybon, A. Adamiecki, P. J. Winzer, S. Randel, L. Salamanca, A. Konczykowska, F. Jorge, J. Y. Dupuy, L. L. Buhl, S. Chandrashekhar, C. Xie, S. Draving, M. Grove, K. Rush, R. Urbanke, High symbol rate coherent optical transmission systems: 80 and 107 Gbaud, J. Lightwave Technol. 32 (2014) 824-831.

[27] T. Xu, J. Li, A. Djupsjöbacka, R. Schatz, G. Jacobsen, S. Popov, Quasi real-time 230-Gbit/s coherent transmission field trial over 820 km SSMF using 57.5-Gbaud dual-polarization QPSK, Tech. Dig. Conf. Asian Commun. Photon. (2013) AF1F.3.

[28] F. Chang, K. Onohara, T. Mizuochi, Forward error correction for 100 G transport networks, IEEE Commun. Mag. 48 (2010) S48-S55.

[29] H. Sun, K.-T. Wu, Clock recovery and jitter sources in coherent transmission systems, Tech. Dig. Conf. Opt. Fiber Commun. (2012) OTh4C.

[30] K. Kikuchi, Clock recovering characteristics of adaptive finite-impulse-response filters in digital coherent optical receivers, Opt. Express 19 (2011) 5611-5619.

[31] R. Kudo, T. Kobayashi, K. Ishihara, Y. Takatori, A. Sano, Y. Miyamoto, Coherent optical single carrier transmission using overlap frequency domain equalization for long-haul optical systems, J. Lightwave Technol. 27 (2009) 3721-3728.

[32] H. Zhang, Y. Cai, D. G. Foursa, A. N. Pilipetskii, Cycle slip mitigation in POLMUX-QPSK modulation, Tech. Dig. Conf. Opt. Fiber Commun. (2011) OMJ7.

[33] A. Bisplinghoff, S. Langenbach, E. S. Vercelli, R. Pastorelli, T. Kupfer, Cycle slip tolerant, differential encoding aware, soft-decision FEC, Tech. Dig. Conf. Opt. Fiber Commun. (2015) Tu3B.2.

[34] P. Poggiolini, G. Bosco, A. Carena, V. Curri, V. Miot, F. Forghieri, Performance dependence on channel baud-rate of PM-QPSK systems over uncompensated links, IEEE Photon. Technol. Lett. 23 (2011) 15-17.

Figure Captions

Fig. 1. Experimental setup and field link of the DP-QPSK coherent transmission over 820 km installed SSMF in Sweden.

Fig. 2. Experimental DP-QPSK I-Q constellations and tributary (I/Q) eye-diagrams before and after 820 km field link (a) 56-Gbaud (b) 57.5-Gbaud.

Fig. 3. Experimental optical spectra of the 56-Gbaud and the 57.5-Gbaud DP-QPSK signals before and after 820 km field link transmission (0.07 nm resolution bandwidth).

Fig. 4. BER performance with different signal launch power in each SSMF span in the 820 km field link.

Fig. 5. BER versus OSNR at the optimum signal launch power (4 dBm for both 56-Gbaud and 57.5-Gbaud signals). The theoretical curve of BER versus OSNR performance is for the 57.5-Gbaud signal.

Fig. 6. Simulation setup for 5-channel quasi-Nyquist spaced DP-QPSK transmission (the 820 km field link is the same as the field link in Fig. 1). CDC: chromatic dispersion compensation, CPE: carrier phase estimation.

Fig. 7. Simulated optical spectra of 5×57.5-Gbaud DP-QPSK Nyquist WDM superchannels before and after 820 km FL transmission.

Fig. 8. BER versus signal launch power in each SSMF span in the field link (simulation).

Fig. 9. BER versus OSNR at the optimum signal launch power in simulation (4 dBm for single-channel transmission with and without NPS, 9 dBm for WDM superchannel transmission). The theoretical curve of BER versus OSNR performance is for the 57.5-Gbaud signal.

Figure01
Click here to download high resolution image

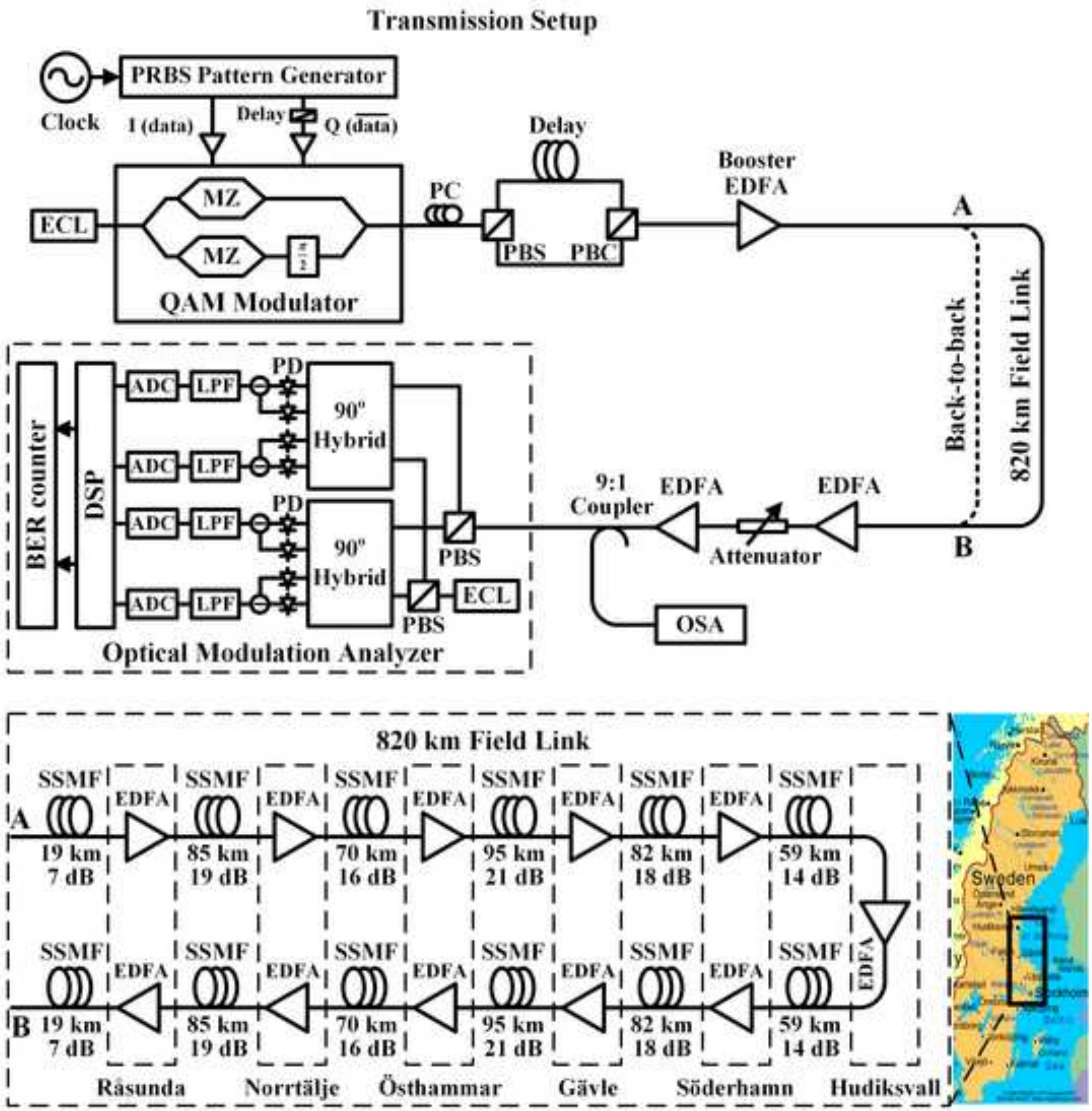

Figure02

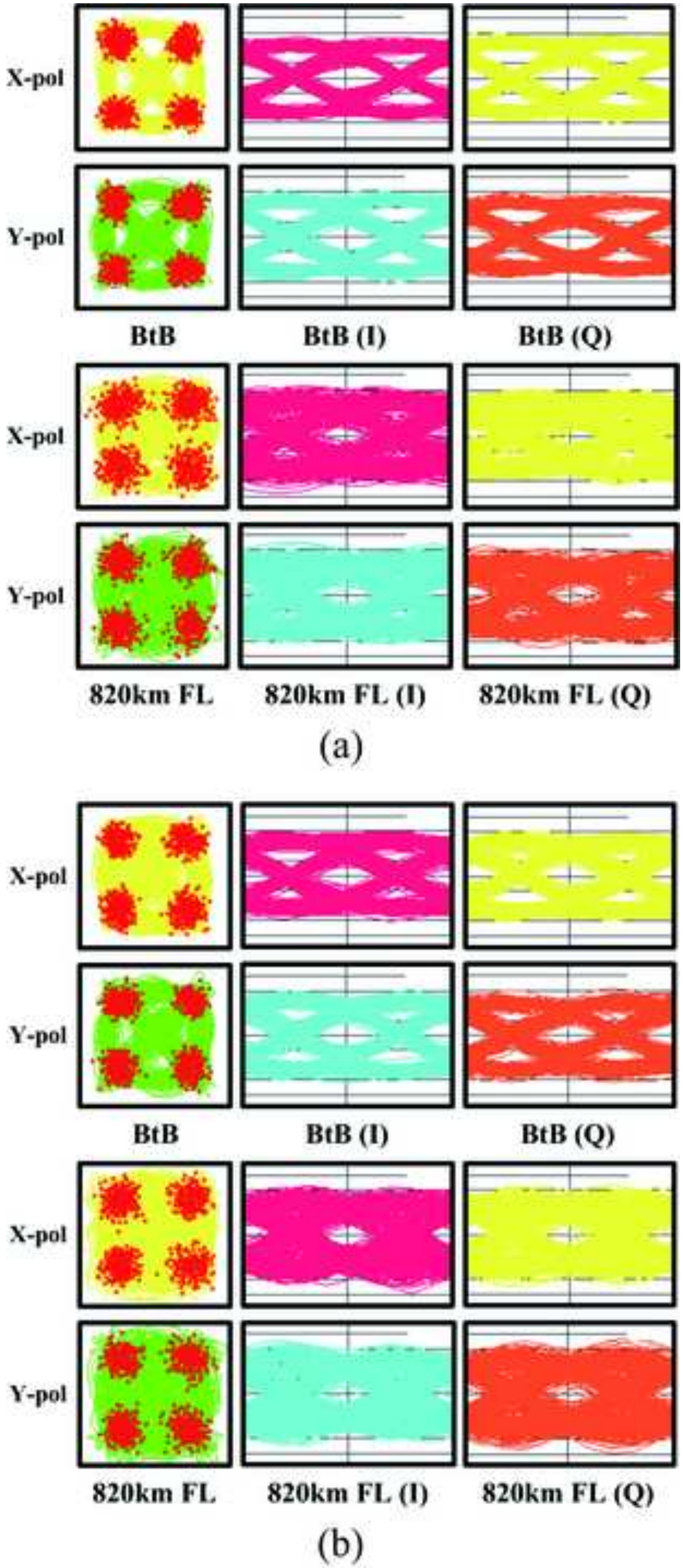
X-pol
Y-pol
BtB
BtB (I)
BtB (Q)
X-pol
Y-pol
820km FL
820km FL (I)
820km FL (Q)
(a)
X-pol
Y-pol
BtB
BtB (I)
BtB (Q)
X-pol
Y-pol
820km FL
820km FL (I)
820km FL (Q)
(b)

Figure03
Click here to download high resolution image

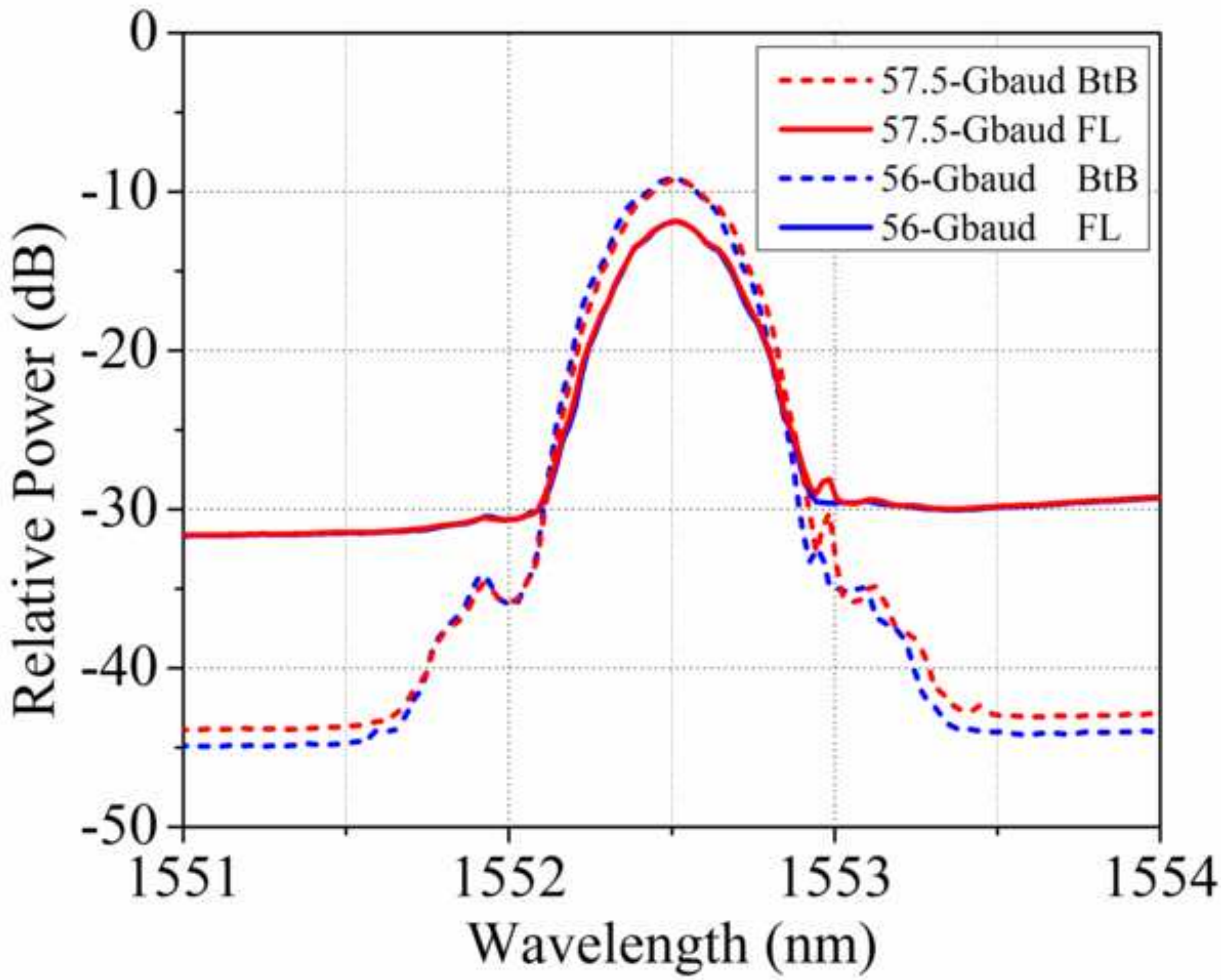

Figure04

Click here to download high resolution image

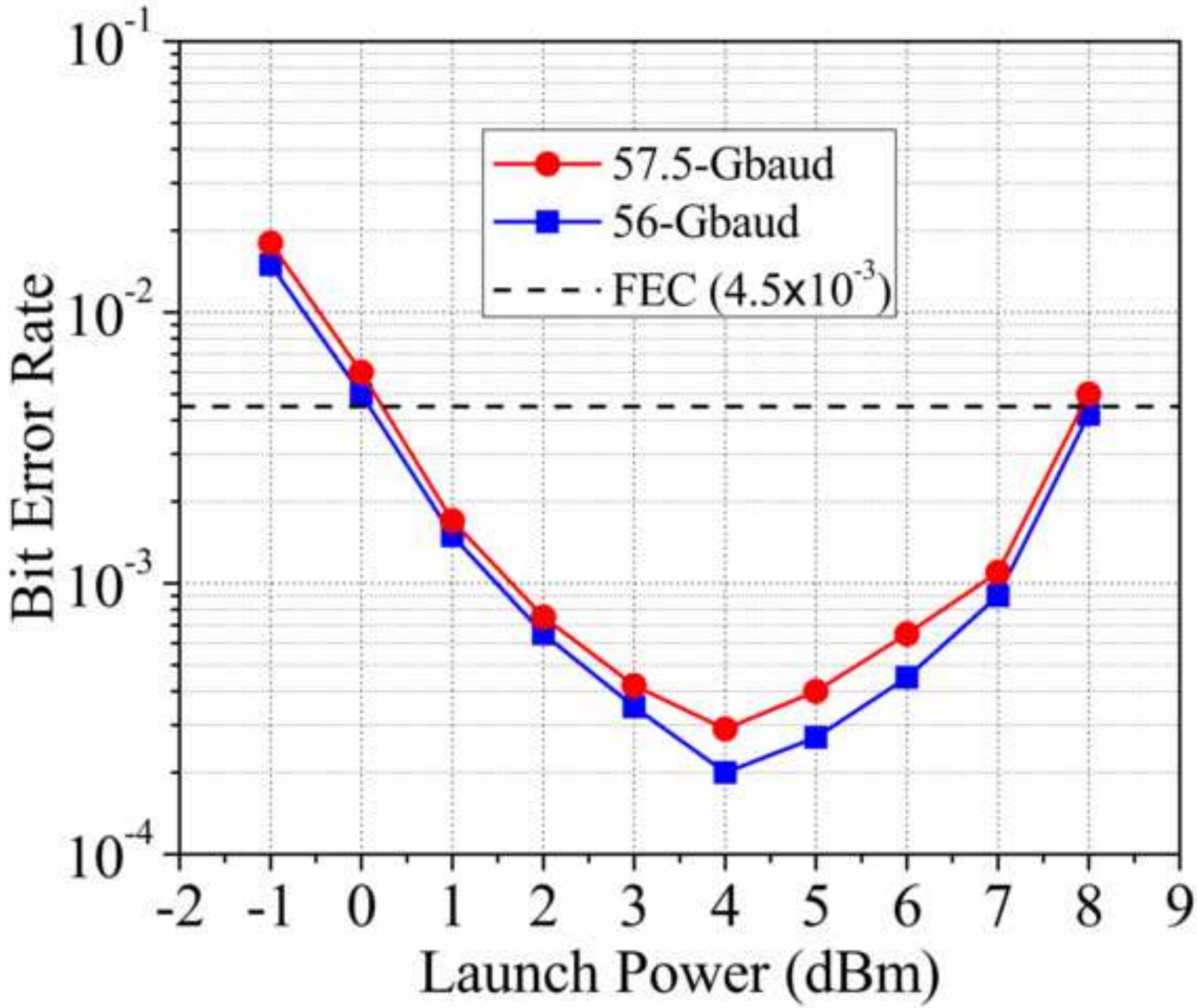

Figure05
Click here to download high resolution image

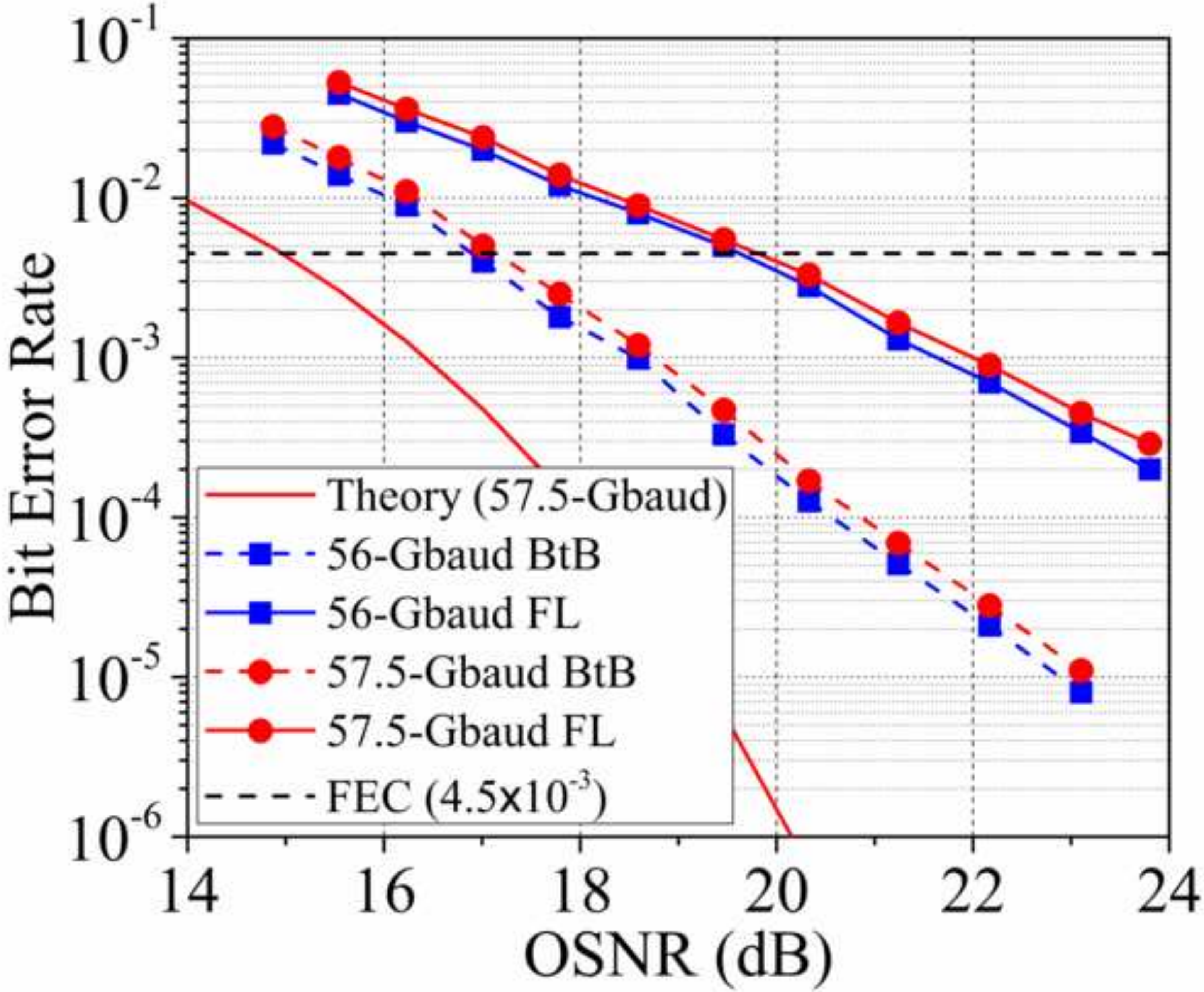

Figure06
Click here to download high resolution image

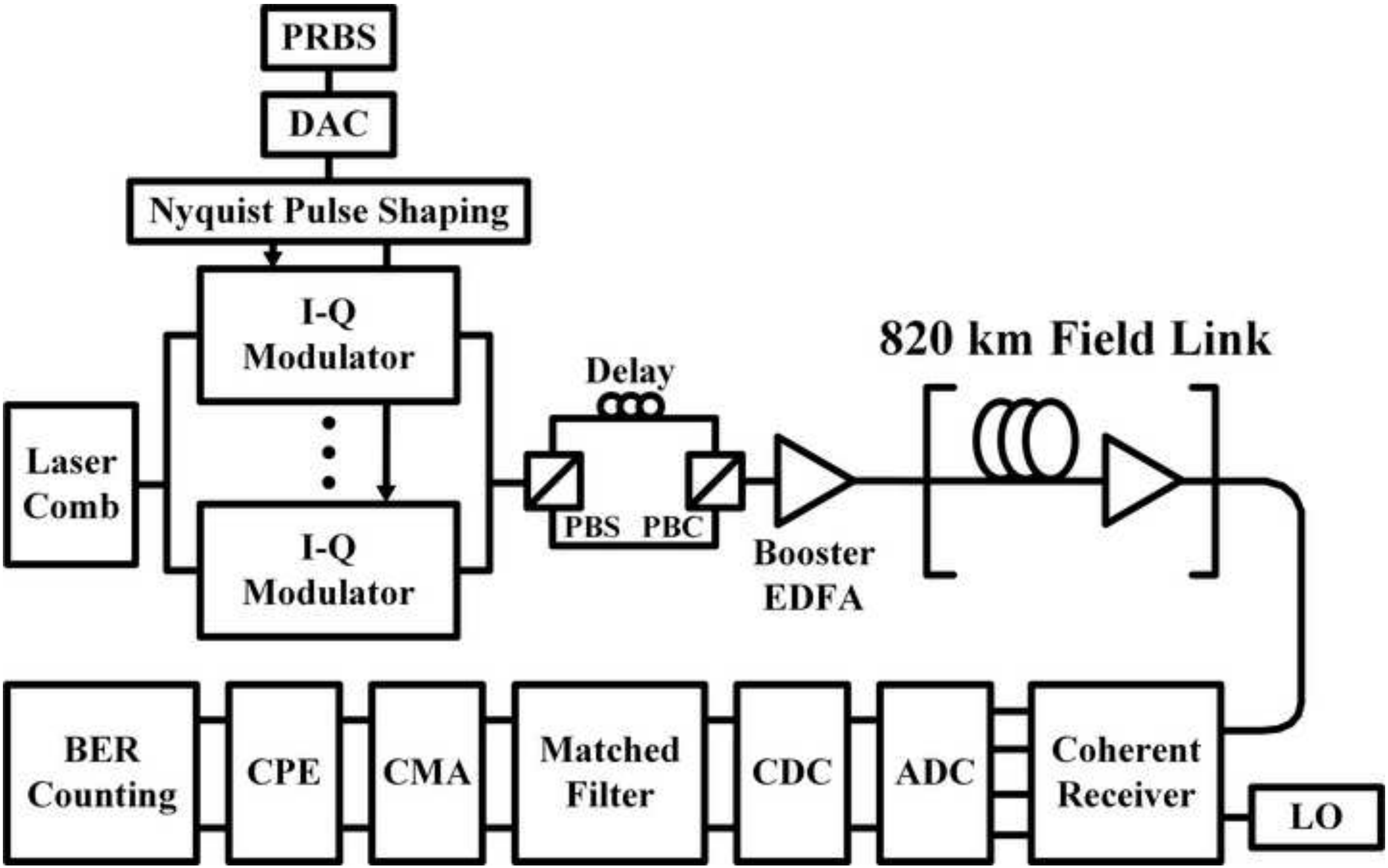

Figure07
Click here to download high resolution image

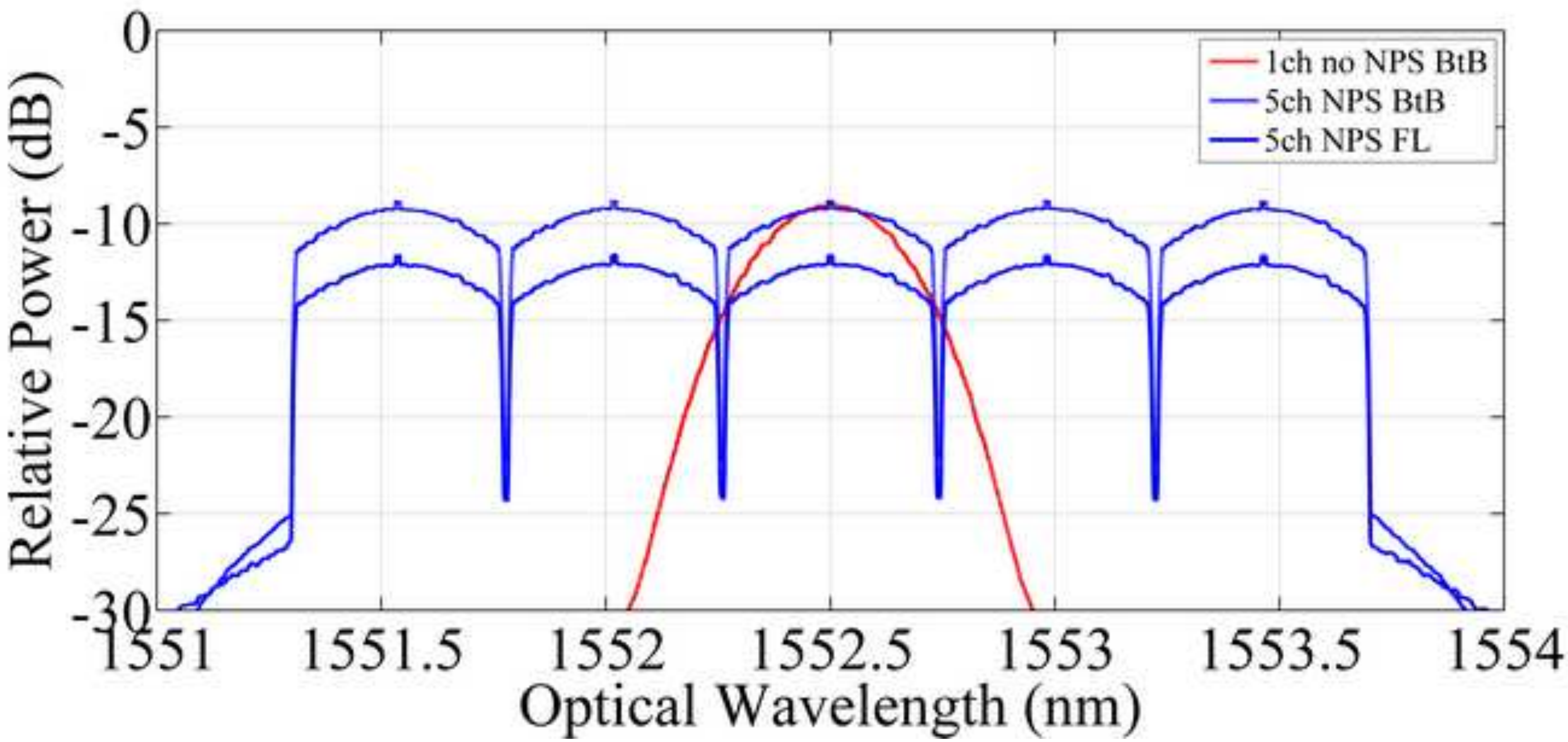

Figure08

Click here to download high resolution image

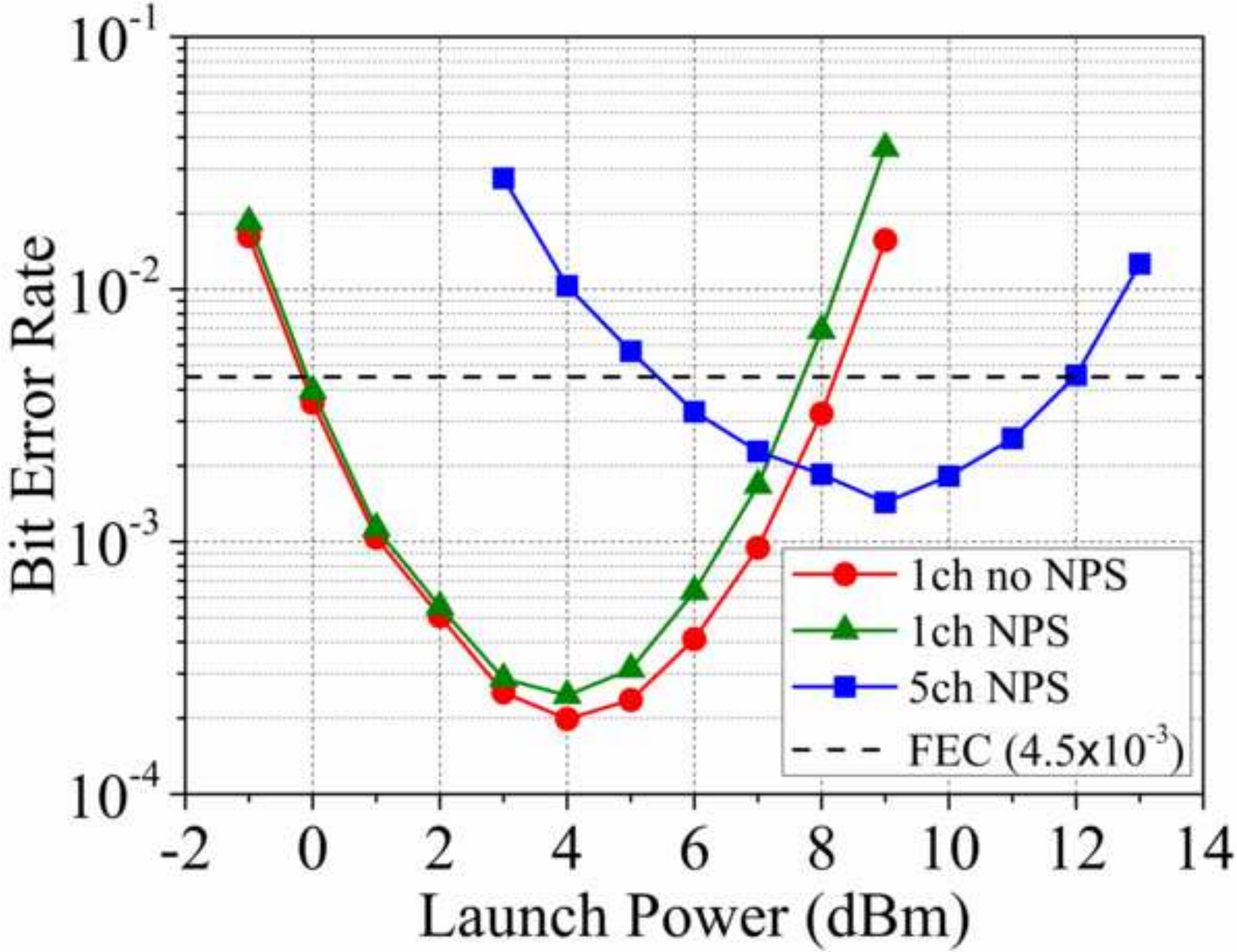

Figure09
Click here to download high resolution image